Available online at www.sciencedirect.com
SCIENCE DIRECT®
Polymer 45 (2004) 919–926
polymer
www.elsevier.com/locate/polymer

Poly(ethylene terephthalate) nanocomposites by in situ interlayer polymerization: the thermo-mechanical properties and morphology of the hybrid fibers

Jin-Hae Chang[a,*], Sung Jong Kim[a], Yong Lak Joo[b], Seungsoon Im[c]

[a]*Department of Polymer Science and Engineering, Kumoh National University of Technology, Kumi 730-701, South Korea*
[b]*School of Chemical and Biomolecular Engineering, Cornell University, Ithaca, NY 14853, USA*
[c]*Department of Fiber and Polymer Engineering, Hanyang University, Seoul 133-791, South Korea*

Received 16 July 2003; received in revised form 3 November 2003; accepted 12 November 2003

Abstract

Nanocomposites of poly(ethylene terephthalate) (PET) with C_{12}PPh–MMT as an organoclay were synthesized by using the in situ interlayer polymerization approach. The PET nanocomposites were melt-spun at different organoclay contents and different draw ratios to produce monofilaments. The thermo-mechanical properties and the morphologies of the PET nanocomposites were examined by using a differential scanning calorimeter, a thermogravimetric analyzer, a wide angle X-ray diffactometer, scanning and transmission electron microscopes, and a universal tensile machine. Some of the clay particles were well dispersed in the PET matrix, and some of them were agglomerated at a size level of greater than approximately 10 nm. The thermal stability and the tensile mechanical properties of the PET hybrid fibers increased with increasing clay content at a DR = 1. However, the values of the ultimate tensile strength and the initial modulus of the hybrid fibers decreased markedly with increasing DR from 1 to 16.

Keywords: PET nanocomposite fibers; In situ interlayer polymerization; Organoclay

1. Introduction

Organic/inorganic nano-scaled composites comprise one of the most important classes of synthetic engineering materials [1–4]. Their makeup is such that they can be transformed into new materials possessing the advantages of both organic materials, such as light-weight, flexibility, and good moldability, and inorganic materials, such as high strength, heat stability, and chemical resistance. The incorporation of organic/inorganic hybrids can result in materials possessing excellent of stiffness, strength and gas barrier properties with far less inorganic content than is used in conventionally filled polymer composites: the higher the degree of delamination in polymer/clay nanocomposites, the greater the enhancement of these properties. Nanocomposites such as these can also be employed as scratch- and abrasive-resistant hard coatings, non-linear optical materials, and reinforcements for elastomers and plastics [5–7].

Several methods have been used to obtain polymer nanocomposites by using organoclays, i.e. solution intercalation, melt intercalation, and in situ interlayer intercalation [8–12]. Among them, in situ interlayer polymerization relies on swelling of the organoclay by the monomer, followed by in situ polymerization initiated thermally or by the addition of a suitable compound. The chain growth in the clay galleries accelerates clay exfoliation and nanocomposite formation. This technique of in situ interlayer polymerization is also particularly attractive due to its versatility and compatibility with reactive monomers and is beginning to be used for commercial applications [13–15].

Poly(ethylene terephthalate) (PET) is a semicrystalline polymer possessing excellent chemical resistance, thermal stability, melt mobility, and spinnability [13–15]. It has been used in such diverse fields as the packaging, electrical, automotive, and construction industries. When PET nanocomposites are prepared, elevated temperatures to, at least,

* Corresponding author.
E-mail address: changjinhae@hanmail.net (J.H. Chang).

0032-3861/$ - see front matter © 2003 Elsevier Ltd. All rights reserved.
doi:10.1016/j.polymer.2003.11.037

above 280 °C are required for in situ intercalation and bulk processing. If the processing temperature is higher than the thermal stability of the organoclay, decomposition will occur, altering the interface between the filler and the matrix polymer. In real processes with organophilic polymers, the interlayer cations are replaced with alkyl ammonium cations to enhance the dispersibility. Since the thermal stability of these kinds of organoclays with alkyl ammonium cations has been a problem, i.e. thermal degradation in the processing of PET above 280 °C, much research has been directed toward the preparation of organoclays that are thermally stable at high temperatures [16–19].

The objective of this study is to evaluate the effect of the organoclay in PET nanocomposites, as a hybrid system, as a function of the amount of organoclay. To obtain the nanocomposites without thermal degradation during the processing, we used a thermally stable organoclay. In this paper, we describe a method for making PET nanocomposites by using in situ interlayer polymerization. Also, the thermo-mechanical properties and the morphologies of PET nanocomposite fibers are reported for different organoclay contents and different draw ratios (DRs).

2. Experimental

2.1. Materials

All reagents were purchased from TCI, Junsei Chemical Co., and Aldrich Chemical Co. Commercially available solvents were purified using distillation.

2.2. Preparation of organoclay: C_{12}PPh–MMT

The organically modified montmorillonite (C_{12}PPh–MMT) used in this study was synthesized using an ion exchange reaction between Na^+–montmorillonite (Na^+–MMT) and dodecyl triphenyl phosphonium chloride ($C_{12}PPh–Cl^-$) [20]. In a 500 mL beaker, 5.0 g (0.02 mol) of bromododecane, 15.8 g (0.06 mol) of triphenyl phosphine, and 300 mL of THF were placed. This solution was heated at 80 °C for 24 h. Then, dodecyltriphenylphosphonium bromide [16], 4.1 g (0.008 mol), was dispersed in a mixture solvent of 120 mL of de-ionized water, 30 mL of ethanol, and 3.0 mL of concentrated HCl at 80 °C. The dispersion of 6.0 g of Na^+–MMT in a 120 mL of water was added to the $C_{12}PPh–Cl^-$ solution, and the mixture was stirred vigorously for 1 h. The precipitate was isolated by filtration, placed in a 500 mL beaker with 300 mL of water and ethanol, and stirred for 1 h. The product was then filtrated and freeze-dried (see Scheme 1).

2.3. Preparation of C_{12}PPh–MMT/PET nanocomposites

All of the samples were prepared as melts. Since the synthetic procedures for all of the hybrids were almost the same, only a representative example, the procedure for the preparation of nanocomposites containing 2 wt% organoclay, is given here. In a polymerization tube, 62 g of 1,2-ethylene glycol (EG) (1.0 mol) and 1.96 g of C_{12}PPh–MMT were placed; the mixture was stirred for 30 min at room temperature. In a separate tube, 97 g of dimethyl terephthalate (DMT) (0.5 mol) and a few drops (1.2×10^{-4} mol) of isopropyl titanate were placed and this mixture was added to the organoclay–EG system, with vigorous stirring to obtain a homogeneously dispersed system. This mixture was heated first for 1 h at 190 °C under a steady stream of N_2 gas. Then, the temperature of the reaction mixture was raised to 230 °C, and that temperature was maintained for 2 h under a steady stream of N_2 gas. During this period, continuous generation of methanol was observed. Finally, the mixture was heated for 2 h at 280 °C at a pressure of 1 Torr. The product redundant was cooled to room temperature, repeatedly washed with water, and dried under a vacuum at 70 °C for 1 day to obtain the PET hybrids. The polymers are soluble in mixed solvents. Therefore, a mixed solvent of phenol/1,1,2,2-tetrachloroethane (TCE) was used in the measurement of solution viscosity. The solution viscosity numbers (see Table 1) range from 0.98 to 1.26. Considering the fact that the clay

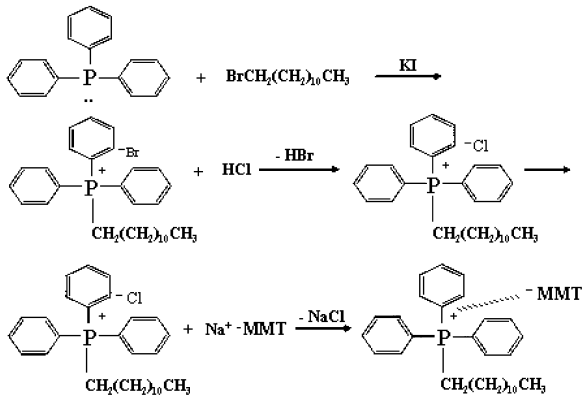

Scheme 1. Synthesis of organoclay.

Table 1
Thermal properties of PET hybrid fibers

Organoclay (wt%)	DR[a]	η_{inh}[b]	T_m (°C)	ΔH_m[c] (J/g)	T_D^i[d] (°C)	wt_R^{600e} (%)
0 (pure PET)	1	1.02	245	32	370	1
1	1	1.26	247	32	375	8
2	1	0.98	245	33	384	15
3	1	1.23	246	32	386	21
3	3		246	31	386	22
3	10		246	31	388	21
3	16		245	31	387	21

[a] Draw ratio.
[b] Inherent viscosities were measured measured at 30 °C by using 0.1 g /100 mL solutions in a phenol/1,1,2,2-tertachloroethane (w/w) mixture.
[c] Enthalpy change of fusion.
[d] Initial weight reduction onset temperature.
[e] Weight percent of residue at 600 °C.

contents excluded out of the polymer, these numbers can be regarded as being reasonably high.

2.4. Extrusion

The composites were pressed at 270 °C, 2500 kg/cm^2 for 2–3 min on a hot press. The ~0.5 mm thick films obtained were dried in a vacuum oven at 110 °C for 24 h; then, they were extruded through the die of a capillary rheometer. The hot extrudates were stretched through a die of capillary rheometer (INSTRON 5460) at 270 °C and immediately drawn at the constant speed of the take-up machine to form fibers with different DRs. The pure PET and PET hybrids were each extruded into fibers through a capillary die with varying DRs, and the thermal properties and the tensile mechanical properties of the extrudates were examined. Standard die diameter (DR = 1) was 0.75 mm. When the organoclay was increased from 0 to 3 wt% in hybrids, all fibers obtained from capillary rheometer were shown bright yellow. The DR was calculated from the ratio of the velocity of extrusion to the take up speed. The mean residence time in the capillary rheometer was ~3–4 min.

2.5. Characterization

The thermal behavior was studied by using a Du Pont model 910 differential scanning calorimeter (DSC) and thermogravimetric analyzer (TGA) at a heating rate of 20 °C/min under a N_2 flow. Wide-angle X-ray diffraction (WAXD) measurements were performed at room temperature by using a Rigaku (D/Max-IIIB) X-ray diffractometer with Ni-filtered Co-Kα radiation. The scanning rate was 2°/min over a range of $2\theta = 2-10°$.

The tensile properties of the fibers were determined using an Instron mechanical tester (Model 5564) at a crosshead speed of 20 mm/min at room temperature. The experimental uncertainties in the tensile strength and the modulus were ± 1 MPa and ± 0.05 GPa, respectively. An average of at least ten individual determinations was obtained.

The morphologies of the fractured surfaces of the extruded fibers were investigated using a Hitachi S-2400 scanning electron microscope (SEM). An SPI sputter coater was used to sputter-coat the fractured surfaces with gold for enhanced conductivity. The samples for the transmission electron microscope (TEM) were prepared by putting PET hybrid fibers into epoxy capsules and then curing the epoxy at 70 °C for 24 h in vacuum. After that, the cured epoxies containing the PET hybrids were microtomed into 90 nm thick slices, and a layer of carbon, about 3 nm thick, was deposited on each slice on a mesh 200 copper net. TEM photographs of ultrathin sections of the polymer/organoclay hybrid samples were taken on a EM 912 OMEGA TEM using an acceleration voltage of 120 kV.

3. Results and discussion

3.1. Wide angle X-ray diffraction

The XRD results for the C_{12}PPh–MMT/PET nanocomposites are shown in the Fig. 1. The d_{001} reflection for the Na^+–MMT was found at $2\theta = 8.60°$, which corresponds to an interlayer distance of 11.99 Å. The XRD peak for the surface-modified clay, C_{12}PPh–MMT, was found at $2\theta = 2.86°$, corresponding to an interlayer distance of 36.08 Å. As expected, the ion exchange between the clay (Na^+–MMT) and the triphenyl phosphine dodecane chloride (C_{12}PPh–Cl^-) resulted in an increase in the basal interlayer spacing in comparison with pristine Na^+–MMT and caused a big shift of the diffraction peak toward lower values of 2θ [20–22]. The organoclay peak was also observed to have $d = 18.20$ Å ($2\theta = 5.65°$), which correlated to the 002 plane of the clay layers.

For PET containing a 1 wt% organoclay content, only slight peak at $d = 17.25$ Å existed in the XRD results for the extrudate fibers. A substantial increase in the intensities of the XRD peaks was observed for clay loadings from 1 to 3 wt%, which suggests that the dispersion is better at a lower clay loading than at a higher clay loading. The presence of the organoclay, however, had no effect on the location of the peak, which indicates that perfect exfoliation of the clay layer structure of the organoclay in PET does not occur [23]. For PET hybrids, the reason the main peak at $2\theta = 2.86°$ disappeared is thought to be due to the peak of the swollen organoclay inserted as polymer chains having a lower diffraction peak than 2°.

Fig. 2 shows the XRD results of the PET nanocomposites containing 3 wt% C_{12}PPh–MMT at various DRs. When the DR was increased from 3 to 16, no obvious clay peaks appeared. This absence of peaks is an indication that the clay layers were exfoliated and dispersed homogeneously in the PET matrix [23] and is direct evidence that the C_{12}PPh–MMT/PET systems formed exfoliated nanocomposites. It suggests that higher stretching of the fiber during the

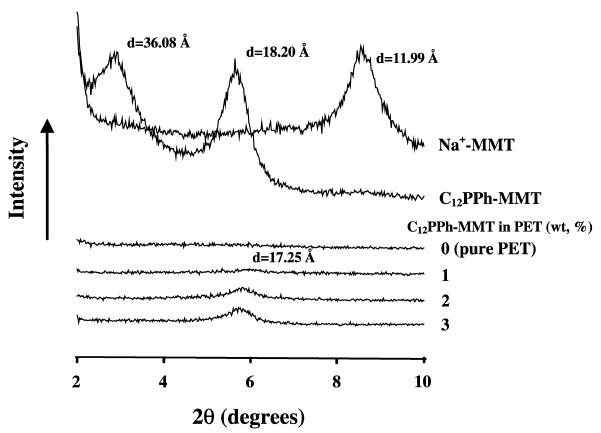

Fig. 1. XRD patterns for clay, organoclay, and PET hybrid fibers with various organoclay contents.

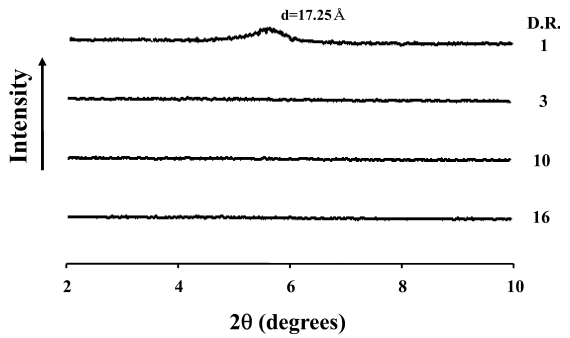

Fig. 2. XRD patterns of 3 wt% C_{12}PPh–MMT in PET hybrid fibers with different draw ratios.

extrusion leads to better dispersion of the clay and this causes exfoliated morphology. Although XRD is most useful in measuring the *d*-spacing of ordered immiscible and ordered intercalated polymer nanocomposites, it may be insufficient for analyzing disordered and exfoliated materials with no peaks.

3.2. Morphology

The clay dispersion in a PET matrix was crosschecked further by using electron microscope data. Electron microscopy and XRD are complimentary techniques and can fill in the gaps in information that other techniques cannot [19,23]. The morphologies of the extruded fibers obtained from hybrid systems containing up to 3 wt% C_{12}PPh–MMT in a PET matrix were examined by observing their fracture surfaces by using a SEM, and the results are in Figs. 3 and 4. Fig. 3 shows that clay phases were formed in an undrawn hybrid fiber with increasing organoclay from 0 to 3 wt%. The PET hybrid fibers with 0–3 wt% C_{12}PPh–MMT showed morphologies consisting of clay domains, 100–150 nm in size, well dispersed in a continuous PET phase. Fig. 4 show micrographs taken of the 3 wt% C_{12}PPh–MMT/PET hybrid fiber obtained at different DRs from 1 to 16. The 3 wt% hybrid fiber with a DR = 3 contained fine clay phases 80–100 nm in diameter (see Fig. 4(b)). The hybrid fiber with a DR = 16 also showed fine dispersion with domain sizes of 30–50 nm in diameter (see Fig. 4(d)).The domain size of the dispersed clay phase is clearly seen to decrease with increasing DR. This declination in the domain size seems to be the result of excess stretching of the fiber when the extrudates pass through the capillary rheometer.

To examine exactly the dispersion of the clay layers in the fiber hybrids, we carried out TEM studies. A TEM allows a qualitative understanding of the internal structure through direct observation. Typical TEM photographs for hybrids with different organoclays are shown in Figs. 5 and 6. The dark lines are the intersections of 1 nm thick sheet layers. Figs. 5 and 6 show the TEM photographs of 1 and 3 wt% hybrid fibers, respectively. Fig. 5 shows that the organoclay is well dispersed in the polymer matrix at all

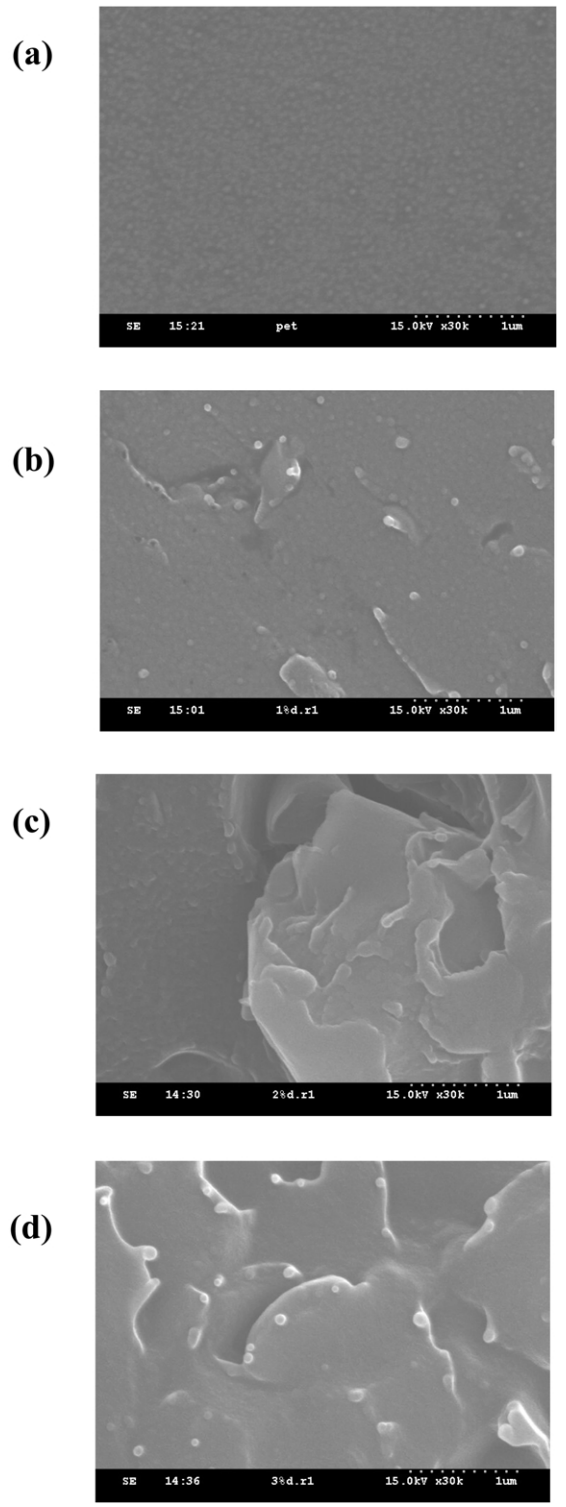

Fig. 3. SEM micrographs of (a) 0 wt% (pure PBT), (b) 1 wt%, (c) 2 wt%, and (d) 3 wt% C_{12}PPh–MMT in PET hybrid fibers.

magnification level, although some parts of agglomerated layers still exist. The existence of peaks in the XRD patterns of these samples should be attributed to these agglomerated layers (see Fig. 1). For the 3 wt% hybrid fiber in Figs. 6(a) and (b), some of the clays are well dispersed in the PET

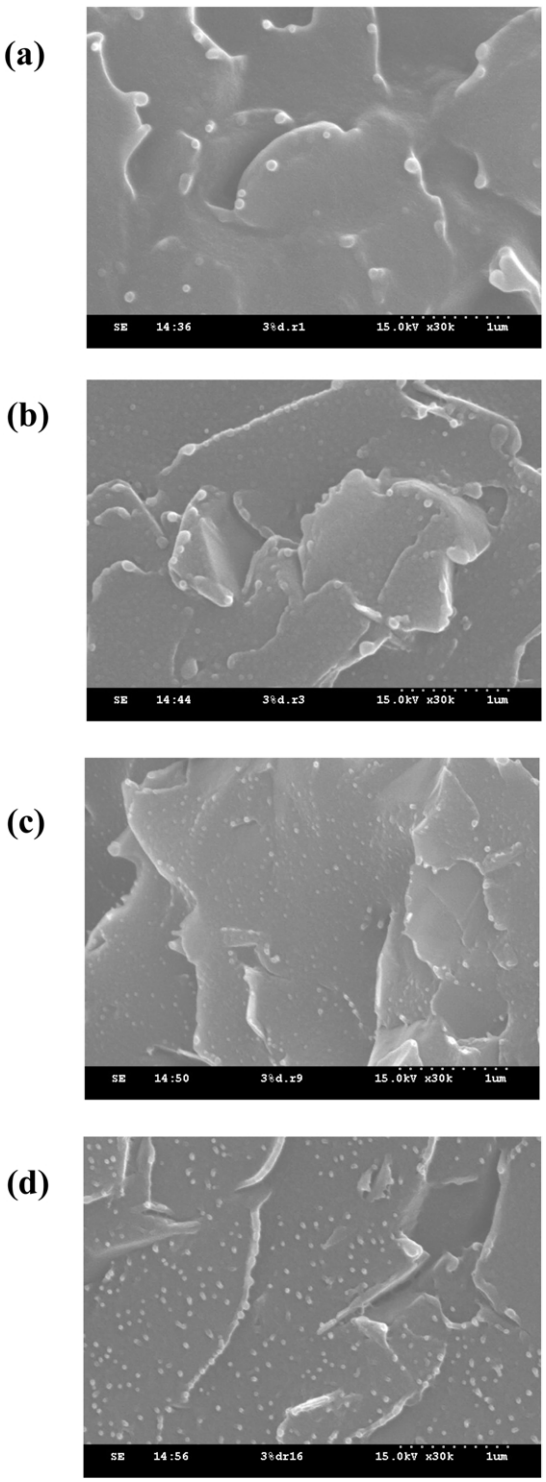

Fig. 4. SEM micrographs of 3 wt% C_{12}PPh–MMT in PET hybrid fibers for draw ratios: (a) 1, (b) 3, (c) 10 and (d) 16.

matrix, and some of them are agglomerated at size levels greater than approximately 10 nm.

On the basis of the preceding results, we can conclude that the state of the clay particles affected the thermal behavior and the tensile mechanical properties for each polymer/clay hybrid. For low clay contents (1 wt%), the

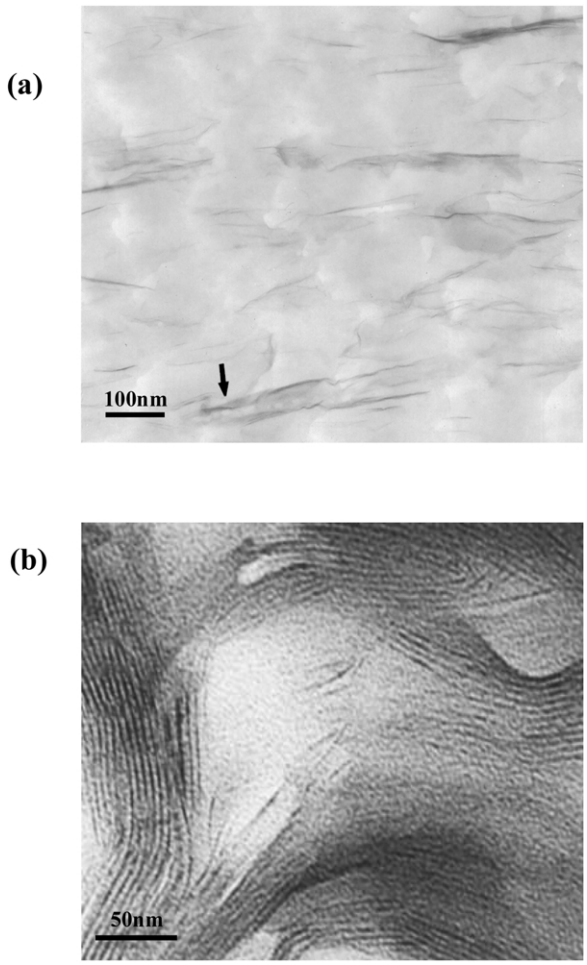

Fig. 5. TEM micrographs of 1 wt% C_{12}PPh–MMT in PET hybrid fibers increasing the magnification levels from (a) to (b).

clay particles may be better dispersed in the matrix polymer without a large agglomeration of particles than they are for high clay contents [24]. However, agglomerated structures form and become denser in the PET matrix above 2 wt% clay content. This is consistent with the XRD observation shown in Fig. 1.

3.3. Thermal behaviors

Table 1 presents the thermal behaviors of pure PET and its nanocomposite fibers obtained by in situ polymerization with different DRs. The endothermic peak of the pure PET appears at 245 °C and corresponds to the melting transition temperature (T_m). Compared with pure PET, the maximum transition peaks of the PET hybrids containing different clay contents were virtually unchanged in the DSC thermograms regardless of the organoclay loading from 1 to 3 wt% at a DR = 1. The heat of fusion (ΔH_m) also remained unchanged, regardless of the organoclay loading at the same DR value. Although the amount of organoclay was increased from 0 to 3 wt%, the values of ΔH_m for all the samples were 32–33 J/g. The melting temperatures and the

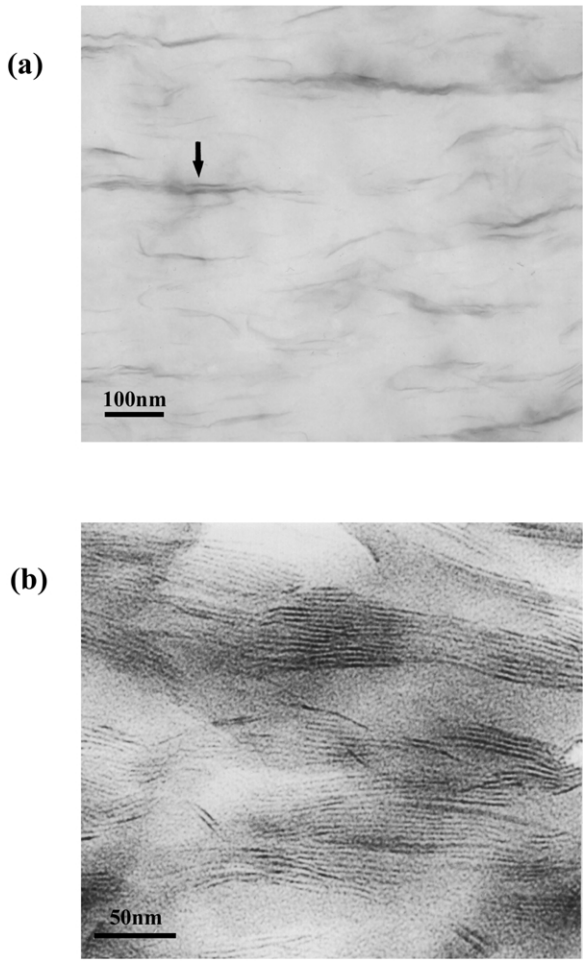

Fig. 6. TEM micrographs of 3 wt% C_{12}PPh–MMT in PET hybrid fibers increasing the magnification levels from (a) to (b).

heats of fusion, in Table 1, of the samples were not affected by the amount of organoclay loading in the PET matrix.

In addition to having the same melting point and endothermic change, the PET hybrids showed improved thermal degradation properties. Comparative TGA results for pure PET and PET hybrids with 0–3 wt% C_{12}PPh–MMT are shown in Table 1 and Fig. 7. Table 1 showed that the initial thermal degradation temperature (T_D^i) of the

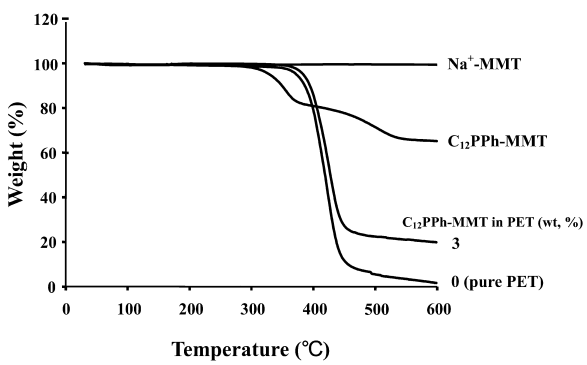

Fig. 7. TGA thermograms of clay, organoclay, and PET hybrid fibers with different organoclay contents.

C_{12}PPh–MMT/PET hybrid fibers increased with the amount of organoclay. T_D^i at a 2% weight loss was observed at 370–386 °C for clay compositions from 0 to 3 wt % in the PET hybrids, with a maximum increase of 16 °C in the case of the 3 wt% C_{12}PPh–MMT/PET as compared to that for pure PET. T_D^i was influenced by the organoclay loading in the hybrid fibers. The weight of the residue at 600 °C increased with clay loading from 0 to 3%, ranging from 1 to 21%. This enhancement of char formation is ascribed to the high heat resistance exerted by the clay itself. For 3 wt% organoclay in the PET hybrid fibers, the overall thermal properties of the PET hybrid fibers were unchanged for DRs from 1 to 16.

Considering the above results, it is perfectly believable that the introduction of inorganic components into organic polymers can improve their thermal stabilities on the basis of the fact that clays have good thermal stability due to the heat insulation effect of the clay layers and to the mass transport barrier to the volatile products generated during decomposition [25,26].

3.4. Mechanical properties

The tensile mechanical properties of pure PET and its hybrid fibers are listed in Table 2. The tensile mechanical properties of C_{12}PPh–MMT/PET hybrid fibers increased with increasing amount of organoclay at DR = 1. When the organoclay was increased from 0 to 3 wt% in hybrids at DR = 1, the strength linearly improved from 46 to 71 MPa. The value of the ultimate strength of the hybrid fiber containing 3 wt% C_{12}PPh–MMT was 1.5 times higher than that of a pure PET fiber.

The same kind of behavior was observed for the initial moduli. For example, the initial tensile modulus of the fiber

Table 2
Tensile properties of PET hybrid fibers

Organoclay (wt%)	DR[a]	Ult. str. (MPa)	Ini. mod. (GPa)	E.B.[b] (%)
0 (pure PET)	1	46	2.21	3
	3	47	2.24	3
	10	51	2.28	3
	16	51	2.39	2
1	1	58	2.88	3
	3	56	2.80	3
	10	50	2.63	3
	16	48	2.47	3
2	1	68	3.31	3
	3	55	2.63	3
	10	54	2.51	3
	16	51	2.29	3
3	1	71	4.10	3
	3	68	3.40	3
	10	62	3.12	2
	16	55	3.08	3

[a] Draw ratio.
[b] Elongation percent at break.

with 2 wt% organoclay was 3.31 GPa, which was about 150% higher than the modulus of pure PET. When the organoclay in PET reached 3 wt%, the modulus had increased about 2.0 fold (4.10 GPa) over that of pure PET. This large increase in the tensile property of hybrid fibers owing to the presence of organoclay can be explained as follows: the amount of increase in the tensile property due to the clay layers depends on interactions between PET molecules and layered organoclays and on the rigid nature of the clay layers. Moreover, the clay is much more rigid than the PET molecules and does not deform or relax as much as the PET molecules do. This improvement was possible because organoclay layers could be dispersed and intercalated in the PET matrix. This is consistent with the general observation that the introduction of organoclay into a matrix polymer increases its strength and modulus [20,24,27–29].

The increases in the tensile strength and the initial modulus with different DRs were insignificant for pure PET, as is usually the case for flexible coil-like polymers. For pure PET, Table 2, the strength and the modulus increased from 46 to 51 MPa and 2.21 to 2.39 GPa, respectively, as the draw ratio was increased from 1 to 16. As Table 2 shows, the values of the ultimate strength and the initial modulus of the hybrid fibers decreased markedly with increasing DR. For 2 wt% of C_{12}PPh–MMT in the hybrid fiber, for example, when the DR was increased from 1 to 16, the tensile strength and the initial modulus values decreased from 68 to 51 MPa and from 3.31 to 2.29 GPa, respectively. Similar trends were observed for 1 and 3 wt% of C_{12}PPh–MMT in the hybrid fiber. The values of the ultimate strength and the initial modulus versus the draw ratio are shown in Figs. 8 and 9, respectively. Similar trends were observed in all of our system with increasing DRs.

An increase in the mechanical tensile strength with increasing DR is very common for engineering plastics and is usually observed in flexible coil-like polymers [30,31]. However, our system did not follow this trend. We suggest that higher stretching of the fiber leads to debonding and

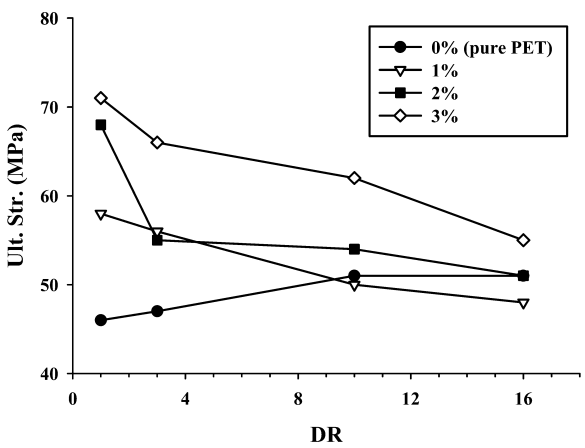

Fig. 8. Effects of draw ratio on the ultimate tensile strength of organoclay contents.

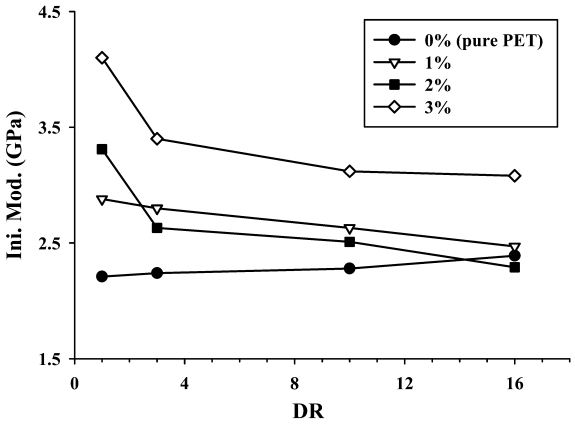

Fig. 9. Effects of draw ratio on the initial tensile modulus of organoclay contents.

voids in the hybrids, which reduce the tensile mechanical properties. This indicates that hydrostatic elongation during the extrusion and the compression molding operations resulted in a debonding in the polymer chain itself and in void formation around the polymer–clay interfaces. Similar observations have been reported by many research groups [32–34], who reported that an imperfect inclusion/matrix interface cannot sustain the large interfacial shear stress that develops as a result of the applied strain. This usually causes yielding or debonding, or both, to occur at or near the interface. Such inelastic deformation relaxes the interfacial shear stress. The result of this smaller interfacial stress is a slower build-up of the normal stress in the inclusion. Because of imperfect bonding, debonding occurs at the interface, giving rise to a constant interfacial shear stress when strain is applied to the composite. Although the electron microscopes have been used many times to prove that no XRD peaks exist (Fig. 2) and that voids form due to debonding caused by increasing the DR from 3 to 16, we, unfortunately, obtained the same morphological results at DR = 1 (see Figs. 3, 5 and 6). The percent elongation at break also changed from 2 to 3% as the DR was increased from 1 to 16.

4. Conclusion

We studied PET nanocomposite fibers made from monomers and organoclay via an in situ interlayer polymerization method. Nano-hybrid fibers were examined to compare the influences of the clay content, the different DRs, the dispersion, and the intercalation states. A reinforcement effect of the organoclay was observed in the thermo-mechanical properties and the morphologies. Especially, the results showed that the mechanical property depended on the organoclay content in the polymer matrix and on the values of the DRs in melt-spinning.

Overall, additions of small amounts of C_{12}PPh–MMT were found to be enough to improve the thermal stability

and the tensile mechanical properties of PET hybrid fibers. Also, when the DR was increased from 1 to 16, the organoclay in the PET caused significant decreases in the values of the ultimate tensile strength and the initial modulus due to debonding around the polymer–clay interfaces and void formation.

References

[1] Giannelis EP. Adv Mater 1996;8:29.
[2] Messersmith PB, Giannelis EP. Chem Mater 1993;5:1064.
[3] Pinnavaia TJ. Science 1983;220:365.
[4] Gilman JW. Appl Clay Sci 1999;15:31.
[5] Wang Z, Lan T, Pinnavaia TJ. Chem Mater 1996;8:2200.
[6] Chang JH, An YU, Sur GS. J Polym Sci, Part B: Polym Phys 2003;41: 94.
[7] Akelah A, Moet A. J Mater Sci 1996;31:3589.
[8] Greenland DG. J Colloid Sci 1963;18:647.
[9] Chang JH, Park KM. Polym Eng Sci 2001;41:2226.
[10] Vaia RA, Ishii H, Giannelis EP. Adv Mater 1996;8:29.
[11] Vaia RA, Jandt KD, Kramer EJ, Giannelis EP. Macromolecules 1995; 28:8080.
[12] Fukushima Y, Okada A, Kawasumi M, Kurauchi T, Kamigaito O. Clay Miner 1988;23:27.
[13] Hwang SH, Paeng SW, Kim JY, Huh W. Polym Bull 2003;49:329.
[14] Wang D, Zhu J, Yao Q, Wilkie CA. Chem Mater 2002;14:3837.
[15] LeBaron PC, Wang Z, Pinnavaia TJ. Appl Clay Sci 1999;12:11.
[16] Zhu J, Morgan AB, Lamelas FJ, Wilkie CA. Chem Mater 2001;13: 3774.
[17] Zhu J, Uhl FM, Morgan AB, Wilkie CA. Chem Mater 2001;13:4649.
[18] Saujanya C, Imai Y, Tateyama H. Polym Bull 2002;49:69.
[19] Davis CH, Mathias LJ, Gilman JW, Schiraldi DA, Shields JR, Trulove P, Sutto TE, Delong HC. J Polym Sci, Part B: Polym Phys 2002;40: 2661.
[20] Chang JH, An YU. J Polym Sci, Part B: Polym Phys 2002;40:670.
[21] Hsiao SH, Liou GS, Chang LM. J Appl Polym Sci 2001;80:2067.
[22] Ke Y, Lu J, Yi X, Zhao J, Qi Z. J Appl Polym Sci 2000;78:808.
[23] Morgan AB, Gilman JW. J Appl Polym Sci 2003;87:1329.
[24] Chang JH, Park DK, Ihn KJ. J Appl Polym Sci 2002;84:2294.
[25] Chang JH, Seo BS, Hwang DH. Polymer 2002;43:2969.
[26] Fornes TD, Yoon PJ, Hunter DL, Keskkula H, Paul DR. Polymer 2002;43:5915.
[27] Lan T, Pinnavaia TJ. Chem Mater 1994;6:2216.
[28] Masenelli-Varlot K, Reynaud E, Vigier G, Varlet J. J Polym Sci, Part B: Polym Phys 2002;40:272.
[29] Yano K, Usuki A, Okada A. J Polym Sci, Part A: Polym Chem 1997; 35:2289.
[30] La Mantia FP, Valenza A, Paci M, Magagnini PL. J Appl Polym Sci 1989;38:583.
[31] Chang JH, Jo BY. J Appl Polym Sci 1996;60:939.
[32] Chawla KK. Composite materials science and engineering. New York: Springer; 1987.
[33] Curtin WA. J Am Ceram Soc 1991;74:2837.
[34] Shia D, Hui Y, Burnside SD, Giannelis EP. Polym Eng Sci 1987;27: 887.